Check for updates

ChemPhysChem

Research Article
doi.org/10.1002/cphc.202300003

Chemistry Europe
European Chemical Societies Publishing

www.chemphyschem.org

Electrostatic Fields Stimulate Absorption of Small Neutral Molecules in Gradient Polyelectrolyte Brushes

Leon A. Smook*[a] and Sissi de Beer[a]

Molecules can partition from a solution into a polymer coating, leading to a local enrichment. If one can control this enrichment via external stimuli, one can implement such coatings in novel separation technologies. Unfortunately, these coatings are often resource intensive as they require stimuli in the form changes of bulk solvent conditions such as acidity, temperature, or ionic strength. Electrically driven separation technology may provide an appealing alternative, as this will allow local, surface-bound stimuli instead of system-wide bulk stimuli to induce responsiveness. Therefore, we investigate via coarse grained molecular dynamics simulations the possibility of using coatings with charged moieties, specifically gradient polyelectrolyte brushes, to control the enrichment of the neutral target molecules near the surface with applied electric fields. We find that targets which interact more strongly with the brush show both more absorption and a larger modulation by electric fields. For the strongest interactions evaluated in this work, we obtained absorption changes of over 300% between the collapsed and extended state of the coating.

Introduction

Under favorable conditions, molecules can absorb from a dilute solution or vapor phase into a polymer brush.[1–7] This local enrichment is useful for a variety of applications, especially for sensing and separations.[8–11] For sensing, partitioning into the brush phase may be enough to provide accurate output. For separations, however, partitioning is only a first step in the process as the target also has to be released at a later stage. Therefore, separations based on polymer brushes require reversible control over the partitioning of molecules in this coating.

The chemical character of the target, in combination with the physical and molecular structure of a polymer brush, has a strong influence on the absorption behavior of targets in these coatings.[6,12–16] Therefore, if one can control the structure of a brush with an external stimulus, one can influence the partitioning of the target into the coating.[17,18] Additionally, the interaction between the target and solvent can also affect the absorption.[19]

In previous work by others,[20–30] it has been shown that an electric field can change the structure of a polymer brush when this brush contains charged moieties. A variety of charged brushes have been investigated ranging from brushes with only a charged moiety at its free chain-end[20–23] to polyelectrolyte brushes with charged moieties along its entire chain length.[24–30] In these systems, when an attractive potential is applied, the charged monomers are attracted to the substrate, leading to a collapsed configuration. Alternatively, when a repulsive potential is applied, the charged monomers are repelled from the substrate, leading to a stretched configuration. We hypothesize that such electrically driven brush reorganization can change the absorption of target molecules in the coating.

Here, we focus on the separation of small amounts of hydrophobic molecules from an aqueous solution. In order to efficiently partition these molecules into a surface coating, this coating must have a similar hydrophobic character since hydrophobic interactions tend to dominate such partitioning.[31] Unfortunately, polyelectrolytes are generally hydrophilic due to its charged moieties, hence simple polyelectrolyte brushes are not expected to absorb much target. Instead, we can design the polymer brush based on a hydrophobic polymer to which we add charged moieties.

As long as the brush contains charged moieties, it should respond to external electric fields. This leaves us with a wide variety of brush architectures to explore. In this work, we choose to focus on gradient polyelectrolyte brushes (Figure 1) instead of end-charged polymer brushes, polyelectrolyte

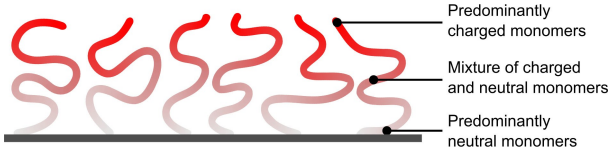

Figure 1. Graphical representation of the gradient polyelectrolyte brushes studied in this work. The composition of the polymer chains gradually changes from neutral to charged from the grafted end to the free end following an exponential gradient. On average 14% of the monomers carry a positive charge.

[a] L. A. Smook, Dr. S. de Beer
Sustainable Polymer Chemistry
Department of Molecules and Materials
MESA + Institute for Nanotechnology
University of Twente
The Netherlands
E-mail: l.a.smook@utwente.nl

© 2023 The Authors. ChemPhysChem published by Wiley-VCH GmbH. This is an open access article under the terms of the Creative Commons Attribution License, which permits use, distribution and reproduction in any medium, provided the original work is properly cited.

© 2023 The Authors. ChemPhysChem published by Wiley-VCH GmbH

14397641, 2023, 9, Downloaded from https://chemistry-europe.onlinelibrary.wiley.com/doi/10.1002/cphc.202300003 by University Of Twente Finance Department, Wiley Online Library on [05/12/2023]. See the Terms and Conditions (https://onlinelibrary.wiley.com/terms-and-conditions) on Wiley Online Library for rules of use; OA articles are governed by the applicable Creative Commons License

brushes, or random polyelectrolyte brushes for the following reasons.

First, end-charged brushes contain only one charged moiety at its free chain end and all responsiveness results from the interaction between this moiety and an electric field. When this system collapses, it will form loops,[20] leading an effective grafting density of roughly twice the original grafting density. Therefore, the modulation of this architecture is limited. For gradient polyelectrolyte brushes, however, more charged moieties are present in the chains, also closer to the grafting point, that can pull the chain towards the grafting plane, leading to a larger window of brush densities.

Second, pure polyelectrolyte brushes do not contain hydrophobic moieties that would interact with the target molecule. Additionally, even in the case of hydrophobic polyelectrolytes, these coatings contain a large number of charges per grafted area. To achieve complete switching of these brushes, we expect to need large electric fields, possibly larger than practically feasible. With a copolymer of charged and neutral moieties, we can introduce absorption sites and limit the grafted charge, while still having a fully responsive system.

Finally, that leaves the different copolymer architectures of charged and neutral monomers: a random, gradient, or diblock copolymer. The diblock copolymer brush has similar issues as the end-charged brush, leaving the random and gradient copolymer brushes as possibilities. We choose gradient copolymers in our simulations as this polymer is easier to synthesize in a one-pot synthesis when the monomers have different reactivities.[32–35] By choosing monomers with different reactivities, one can synthesize such gradient polyelectrolyte brushes using conventional grafting from and grafting to approaches.

Here, we investigate these gradient polyelectrolyte brushes (GPEBs) via coarse-grained molecular dynamics simulations in an implicit poor solvent for all monomer and target particles. Figure 1 shows a graphical representation of this system. We expose these brushes to a Lennard–Jones target which also experiences implicit poor solvent conditions. In order to evaluate the ability of our system to modulate the amount of absorbed target, we test whether an electric potential affects the sorption of this target into this coating. Additionally, we vary the interaction strengths of the target with itself and the polymer to see how this affects its partitioning. We expect that the coatings absorb less target in the collapsed state than in the stretched state and that this effect is stronger for stronger interactions between the target and coating.

Results and Discussion

With molecular dynamics simulations, we investigate the sorption behavior of gradient polyelectrolyte brushes, where the charge distribution along the polyelectrolyte chains follows an exponential gradient. The remainder of this paper is structured as follows. First, we investigate the sorption behavior for Lennard–Jones particles at a low concentration ($\mu_s^* = -7.0$)[1,2] and we vary the affinity of these particles with the monomers in comparison to a fixed polymer self-interaction between the charged and neutral monomers ($\varepsilon_{p,p} = 1.0$). Then, we expose these brushes to different external fields ($-15 < E^* < 15$)[3] and see how this affects the absorption behavior. We note that the electric field strengths in this work are larger than those used in most empirical experiments, when they are converted to real units. Such strong electric fields are required to generate a signal over the thermal noise in the simulation (see also the discussion in Ref. [30]). While our fields are larger than most experimental setups, they are still smaller than the field strengths required to decompose water.[36]

Sorption in Gradient Polyelectrolyte Brushes

After exposing the gradient polyelectrolyte brushes to the Lennard–Jones target, we extract density profiles for all components in the simulation. Figure 2 displays these density profiles, with the polymer density profile displayed in the top panel, the charged monomer density profiles in the middle panel, and the target density profiles in bottom panel. These simulations were performed in the absence of an electric field (i.e. $E^* = 0$).

Under all tested conditions, the structure of the brush is similar as is shown in the polymer density profiles in Figure 2 (top panel). For all polymer-target interaction strengths, the polymer density profile shows characteristics that are similar to homopolyelectrolyte brushes[24,28] with a parabolic profile at low z-values and a long tail at higher z-values; the system can reduce its free energy by spreading the charged monomers over a larger volume. This spreading of charged monomers induces a slight pulling force on the brush, leading to a lower density near the grafting plane when compared to neutral brushes in poor solvent conditions.[6]

Additionally, we observe an interesting structure in the density profile of the charged monomers (Figure 2, middle panel). While the distribution of monomers along the length the polymer chains follow an exponential distribution with a maximum at the free chain end, the distribution in the brush displays a bimodal pattern. In order to reduce the unfavorable exposure of neutral monomers to vacuum, a subset of chains is recruited to reduce these unfavorable interfaces on both sides of the brush. The charged monomers and counterions experience a weaker interaction with the neutral monomers than with themselves and hence the system can minimize energy by preferentially exposing these particles at the interfaces. Such an effect has been predicted on the outside of

[1] All values in this work are reported in reduced Lennard–Jones units, unless explicitly stated otherwise.

[2] Subscripts refer to the particle type in the simulation: s – target; p – polymer (both charged and neutral monomers); s|p refers to both target or monomer particles.

[3] Using $\varepsilon = k_B T \approx 25.7$ meV and $\sigma = 1$ nm, the reduced units for the electric field translates to 1 $E^* = 2.5 \times 10^7$ V/m.

© 2023 The Authors. ChemPhysChem published by Wiley-VCH GmbH

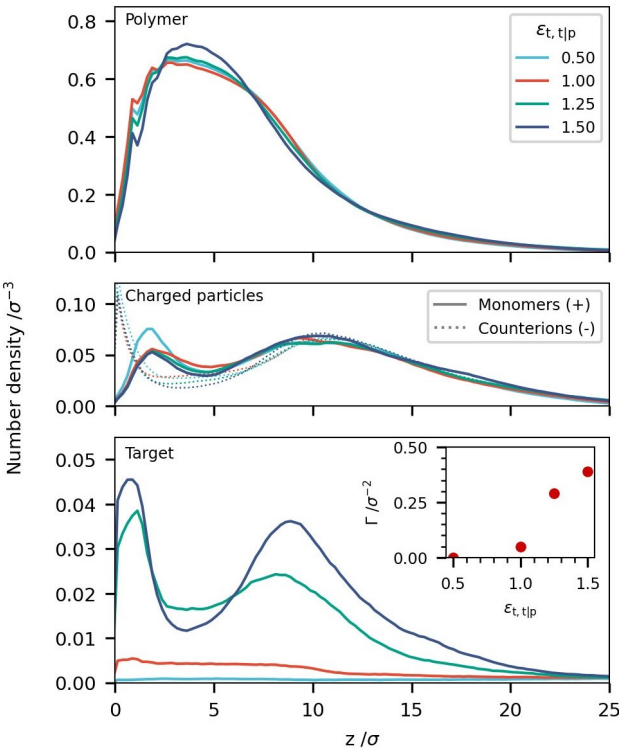

Figure 2. Density profiles of polymer (top panel), charged particles (middle panel), and target (bottom panel) for different target-polymer interaction strengths ($\varepsilon_{t,t|p}$). A stronger interaction leads to an increase in absorbed target. The inset shows the excess sorption (Γ) for different polymer-target interaction strengths. System parameters: $\rho = 0.1\ \sigma^{-2}$, $T^* = 1.0$, $\mu_t^* = -7$, $E^* = 0$.

the brush for physical gradient copolymer brushes with monomers with different solubilities[37] and in gradient copolymer micelles.[38] However, to the best of our knowledge, the secondary maximum we observe has not been reported previously.

While the origin of the maximum close the grafting plane is outside the scope of this manuscript, we hypothesize that this second maximum can result from both enthalpic and entropic effects. Enthalpically, the interaction between counterions and charged monomers and the vacuum is more favorable than that of neutral monomers. Thus, by preferentially exposing the charged entities on both sides of the brush, the system can reduce its free energy. Alternatively, the gradient polyelectrolytes are intrinsically stretched due to intra-chain charged interactions. As a result, an empty depletion zone forms near the grafting plane, which can be filled more efficiently by the smaller counterions. These counterions then form an effective surface charge, which leads to the collapse of some polyelectrolyte chains. In this case, the maximum close to the surface is entropic in origin.

Besides the qualitative similarities in all cases, there are small differences between the brush exposed to the target with the strongest interaction ($\varepsilon_{t,t|p} = 1.50$) and the other brushes. It appears that enough target absorbs to slightly affect the brush structure for this strongly-interacting case, leading to a slightly higher maximum density (0.72 σ^{-3} vs 0.67 σ^{-3}).

The density profiles of the target are presented in the bottom panel of Figure 2. These profiles display absorption maxima at two different z-values when the polymer-target interaction is stronger than the polymer self-interaction ($\varepsilon_{t,t|p} > \varepsilon_{p,p}$). The first maximum is found between the substrate and the densest part of the brush at around $z = 1\ \sigma$; the second maximum is found at slightly higher values ($z = 8.1\ \sigma$ for $\varepsilon_{t,t|p} = 1.25$ and $z = 8.9\ \sigma$ for $\varepsilon_{t,t|p} = 1.50$. Interestingly, these second maxima correspond roughly to a maximum in the density of the charged monomer (middle panel, Figure 2), indicating that these absorbed target particles modulate the interaction between like charges by acting as a spacer. This absorption behavior for strongly-interacting target particles is completely different from what we observed in previous simulations on neutral brushes in a gas (equivalent to a poor solvent) exposed to a Lennard–Jones vapor.[6]

The absorption behavior for weaker interaction strengths ($\varepsilon_{t,t|p} \leq \varepsilon_{p,p}$) display a qualitatively different absorption behavior. For $\varepsilon_{t,t|p} = 0.50$, the target does not absorb at all as the relative interactions between the target and polymer compared to the polymer interaction are not favorable for absorption.[6] Additionally, the absorption energy of the target is not strong enough to counteract the thermal energy. For $\varepsilon_{t,t|p} = 1.00$, the relative interactions are more favorable, but the thermal energy is still significant; the density profile of the target roughly follows that of the polymer. This behavior was previously also observed for brushes exposed to a Lennard–Jones vapor where the interaction strengths between the polymer and polymer and between the polymer and vapor were equivalent.[6]

The qualitative differences in absorption behavior translate into quantitative differences as well. If we consider the surface excess of target particles, that is the number of target particles that are present in the coating in excess of the bulk concentration:

$$\Gamma = \int_0^\infty \langle \phi_s(z) \rangle - \langle \phi_s \rangle_{bulk}\, dz, \tag{1}$$

we can observe these differences (inset Figure 2). For a weakly interacting target ($\varepsilon_{t,t|p} = 0.50$), we find a surface excess (Γ) of 0.00 σ^{-2}, indicating the presence of the coating has no effect on the absorption of target particles. For slightly stronger interacting targets, the surface excess increases from $\Gamma = 0.05\ \sigma^{-2}$ for $\varepsilon_{t,t|p} = 1.00$, to $\Gamma = 0.29\ \sigma^{-2}$ for $\varepsilon_{t,t|p} = 1.25$, to $\Gamma = 0.39\ \sigma^{-2}$ for $\varepsilon_{t,t|p} = 1.50$. Therefore, a stronger interaction between the polymer and the target leads to more absorption. Additionally, we note that this sharp increase around $\varepsilon_{t,t|p} = 1.00$ hints at a phase transition.

© 2023 The Authors. ChemPhysChem published by Wiley-VCH GmbH

14397641, 2023, 9, Downloaded from https://chemistry-europe.onlinelibrary.wiley.com/doi/10.1002/cphc.202300003 by University Of Twente Finance Department, Wiley Online Library on [05/12/2023]. See the Terms and Conditions (https://onlinelibrary.wiley.com/terms-and-conditions) on Wiley Online Library for rules of use; OA articles are governed by the applicable Creative Commons License

Response to Electric Field

The results of the previous section tell us that target particles absorb into gradient polyelectrolyte brushes when no electric field is applied. Now, we will expose these same systems to an external electric field and monitor their response based on the density profiles of the different particles in the simulation. These density profiles are presented in Figure 3 where the density profiles of the polymers is displayed in the first column, that of the charged monomers in the second column, and that of the target in the third column. The different rows present the different applied electric fields ranging from $E^*=-12$ (top row) to $E^*=12$ (bottom row). These density profiles are from simulations with strong polymer-target interactions ($\varepsilon_{t,t|p}=1.50$).

Brush Configuration

Let us first discuss the response of the brush as a result of an external electric field. When we apply a negative potential ($E^*<0$, Figure 3, second row), we observe that the polymer density profile gradually changes from a parabolic profile with a long tail to a rectangular profile with a high maximum density as the strength of the field increases. A stronger negative field (Figure 3, first row) leads to larger attractive forces on the charged monomers, leading to an increasingly collapsed brush.

When we apply a positive potential ($E^*>0$, Figure 3, fourth and fifth row), we observe a similar transition in the opposite direction: The density profile gradually changes into a rectangular profile with a large height and low density as the chains stretch away from the surface. When the chains are fully stretched, the brush density throughout the brush is roughly equal to the grafting density ($\rho=0.1\,\sigma^{-2}$). Here we note that the chains tend to aggregate into pillar-like structures due to the poor solvent conditions (Figure 3, snapshot insets). This pillar-formation has also been observed in simulations of sparser polyelectrolyte brushes in poor solvents.[39,40] Additionally, we observe a non-zero density above a distances equal to the contour length of the chains. This effect results from bonds in some chains that are stretched as a result of the forces acting on the charged moieties.

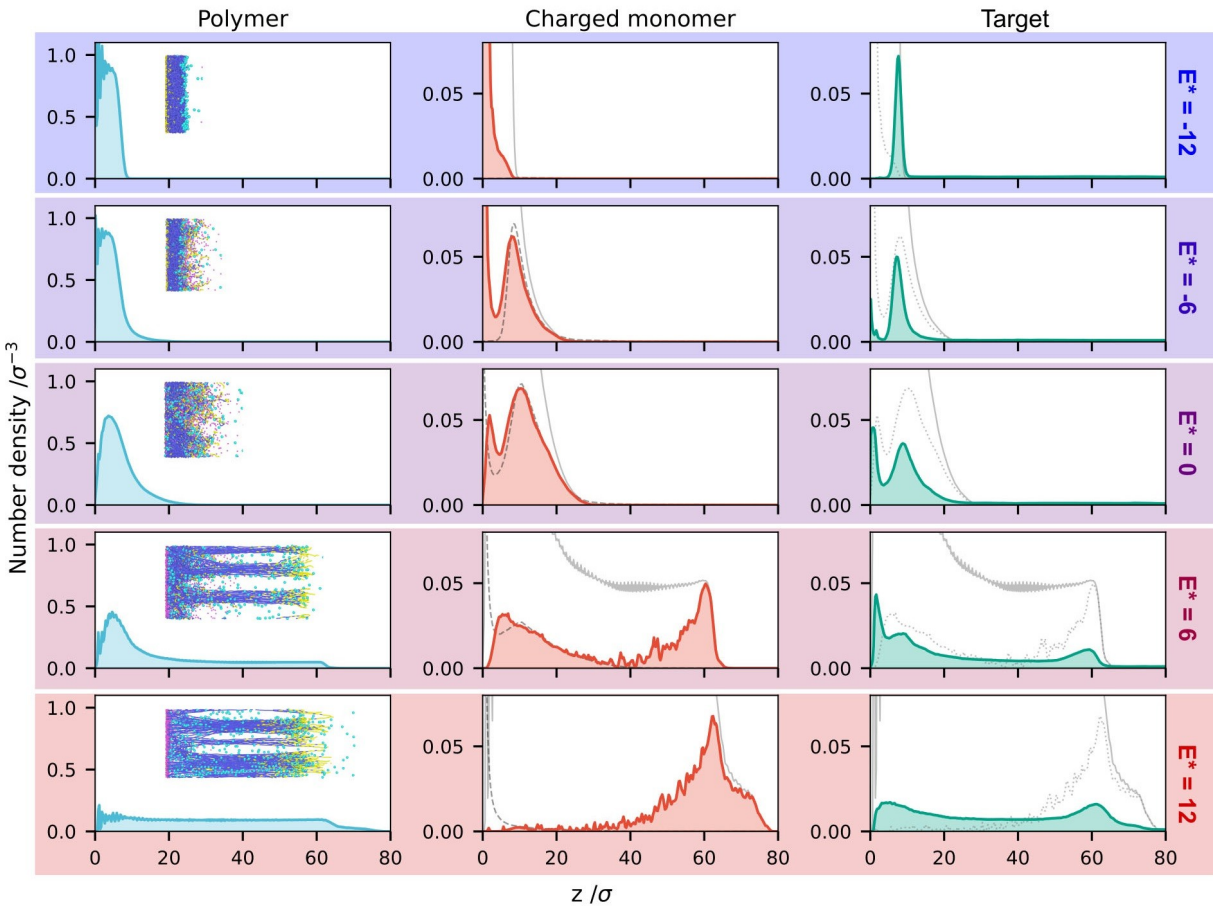

Figure 3. Density profiles of different components of the gradient polyelectrolyte brush systems exposed to a Lennard–Jones target for different electric field strengths. The solid and dashed gray lines in the charged monomer profiles show, respectively, the polymer and counterion profiles for reference. The dotted lines in the target profiles show the charged monomer profiles for reference. $\rho=0.1\,\sigma^{-2}$, $T^*=1.0$, $\mu_t^*=-7$, $\varepsilon_{p,t}=\varepsilon_{t,t}=1.5$.

© 2023 The Authors. ChemPhysChem published by Wiley-VCH GmbH

14397641, 2023, 9, Downloaded from https://chemistry-europe.onlinelibrary.wiley.com/doi/10.1002/cphc.202300003 by University Of Twente Finance Department, Wiley Online Library on [05/12/2023]. See the Terms and Conditions (https://onlinelibrary.wiley.com/terms-and-conditions) on Wiley Online Library for rules of use; OA articles are governed by the applicable Creative Commons License

As an aside, we point out that the density profiles show oscillations at low values for z as is often observed in molecular dynamics simulations of grafted systems due to packing effects close to a fixed boundary. Besides these oscillations, we observe oscillations in the charged monomer profiles under stretched conditions. These oscillations form due to the fact that all chains are grafted at the same height and bond lengths are equal for all bonded beads. As a result, maxima occur at these equilibrium bond distances.

Back to the discussion at hand, if we look at the density profiles of the charged monomers (middle column), we can see that the brushes seem to bifurcate into multiple subpopulations at intermediate, non-zero electric fields. Only a limited number of chains are needed to generate an opposite, equivalent electric field, and the remaining chains experience effectively neutral conditions. This effect is in line with simulations on polyelectrolyte brushes in electric fields[24,27,29] and theoretical free-energy arguments.[26] The bifurcation of the chain states also reflects in the density profiles of the charged monomers in the brushes. Three modes can be seen in the density profiles of the polymer: a collapsed mode (near $z=0\,\sigma$), a relaxed mode (around $z=6$–$10\,\sigma$), and a stretched mode ($z>55\,\sigma$). The presence of an electric field modulates the distribution of the chains over the different modes, leading to a higher population in the collapsed and stretched modes for stronger fields. Besides the redistribution of the chains over the different modes, the positions of the relaxed and stretched modes themselves also shift slightly under influence of the electric field. This shift is mainly the result of two crowding effects: The increasing amount of polymer in this mode leads to steric effects and stretching since the chains in the relaxed mode experience a relatively larger effective grafting density,[29] and in the stretched mode the increasing charge density leads to an additional spreading of the location of the stretched mode.

Effect on Absorption

The restructuring of the brush changes the absorption properties of the coating. To illustrate this change in absorption behavior, we plot the target density profiles for the system with a low concentration ($\mu_s^*=-7.0$) and strong target-polymer interaction ($\varepsilon_{t,t|p}=1.5$) in the right column of Figure 3. Starting from the condition without an electric field ($E^*=0$), we can see that the sorption behavior of the brush changes if an electric field is applied in either direction. For a negative electric field, target particles get expelled from the bulk region due to limited available volume. Similarly, the collapse of more and more chains leads to more polymer at the brush-grafting surface interface, which expels absorbed target at this interface. Under fully collapsed conditions ($E^*\leq -9$), excess target is only present at the brush-target interface in the form of absorbed target and the coating effectively has become a flat surface to which the target has a high affinity.

When an electric field is applied in the opposite direction ($E^*>0$), more and more chains are recruited into the stretched phase. As a result the bulk polymer density in the lower regions of the brush gradually declines and the amount of absorbed target follows this trend. Additionally, the decreased bulk density also deteriorates the grafting plane-polymer interface and this surface adsorption decreases concurrently. Simultaneously, the polymer density at higher distances ($z>50\,\sigma$) increases and is especially rich in charged monomers. As a result, the solvating effect of the target particles leads to a new maximum in the target density profile around $z=60\,\sigma$. Combined with the increased absorption in the volume that was previously unoccupied by the brush, these effects lead to an increased sorption.

This increased sorption is also visible in the surface excess (Γ) for this system under different conditions (Figure 4). In line with the limited sorption we observed previously in the absence of an electric field, the sorption in the system where the polymer-target interactions are weak ($\varepsilon_{t,t|p}=0.50$ and $\varepsilon_{t,t|p}=1.00$) are hardly affected by an electric field. For stronger interactions, however, there is a significant effect on the sorption where the increase goes through a maximum of approximately 112% and 343% compared to the weakest sorption for $\varepsilon_{t,t|p}=1.25$ and $\varepsilon_{t,t|p}=1.50$, respectively.

The trend in surface excess versus the electric field strength can be explained as follows. In a fully collapsed state, the surface excess is mainly due to adsorption onto the brush, giving a nearly constant surface excess with increasing electric field. With a further increase of the electric potential, more and more chains start to relax, giving space for target particles to enter the brush bulk and area between the grafting plane and the brush. Once the field turns positive, the first chains start to stretch, effectively increasing the volume in which interactions can take place. When most chains have been stretched the charged ends of the chain stretch so much that they effectively expel the solvating target. Interestingly, for these stretched conditions, there seems to be a qualitative differences between $\varepsilon_{t,t|p}=1.25$ and $\varepsilon_{t,t|p}=1.50$ in that their

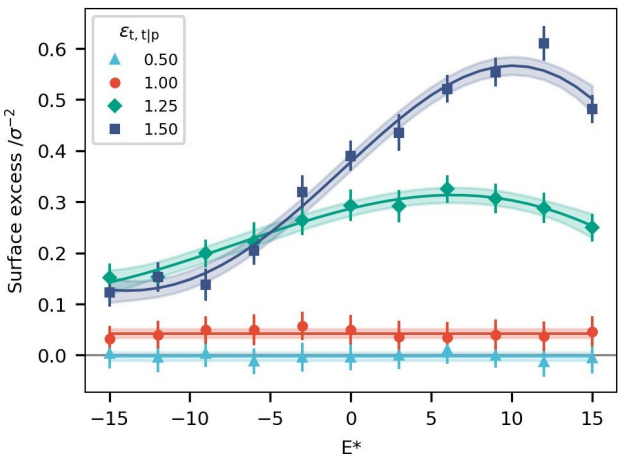

Figure 4. Surface excess of target compared to the bulk concentration. The lines and shaded confidence intervals are a guide to the eye and are constructed by fitting a non-parametric gaussian process model onto the data. $\rho=0.1\,\sigma^{-2}$, $T^*=1.0$, $\mu_t^*=-7$, $\varepsilon_{p,t}=\varepsilon_{t,t}=1.5$.

© 2023 The Authors. ChemPhysChem published by Wiley-VCH GmbH

14397641, 2023, 9, Downloaded from https://chemistry-europe.onlinelibrary.wiley.com/doi/10.1002/cphc.202300003 by University Of Twente Finance Department, Wiley Online Library on [05/12/2023]. See the Terms and Conditions (https://onlinelibrary.wiley.com/terms-and-conditions) on Wiley Online Library for rules of use; OA articles are governed by the applicable Creative Commons License

absorption maxima are at different extensions. This difference is the result of the different types of absorption that play a role in this system: adsorption onto chains and solvating. The former gradually increases as it depends on the volume of the brush. However, the latter gradually decreases as it relates to the number of charge-charge interactions between charged monomers in close proximity. The dependencies of these two types of absorption do not follow a similar trend with respect to an applied electric field, and hence different interaction strengths have different absorption maximum. The different types of sorption can also explain the cross-over around $E^* = -6$ for $\varepsilon_{t,t|p} = 1.25$ and $\varepsilon_{t,t|p} = 1.50$.

The system we investigated can modulate the absorption of a Lennard–Jones target, in some cases with an increase of 343% between the absorption in the collapsed and stretched state. However, in this work, we investigated only the absorption in a single brush with a single target concentration. It is likely that this sorption increase can be enhanced even more if brush parameters are optimized for a specific target. For instance, our trial system has a moderate grafting density of $\rho = 0.1\ \sigma^{-2}$ and a charge fraction $\langle f \rangle = 0.14$. These conditions lead to a brush that can easily switch in response to an electric field, while still being in the brush regime. However, especially in the stretched state, the polymer density over the entire brush height is quite limited ($0.1\ \sigma^{-3}$) as it is directly correlated with the grafting density. As a result, the particles in the simulation do not completely fill the available volume. Therefore, we hypothesize that the absorption modulation can be significantly improved if brush parameters are optimized for a specific target, so that in the ideal case the polymer and target form a space-filling layer in the extended state and fully collapsed state. Similarly, we expect that the charge fraction of the brush also affects the magnitude of this modulation: A higher charge fraction means that more charge interactions have to be modulated, which would lead to more absorption. Simultaneously, more charge also requires a stronger electric field to achieve switching, which would limit the modulation capacity. In future work, we intend to explore how absorption modulation relates to the brush properties for a given target, how these optimal conditions differ for different types of targets, and how these differences might be exploited for separations.

Conclusion

We performed molecular dynamics simulations on gradient polyelectrolyte brushes under different conditions. Electric fields cause the brush to change its configuration into a more stretched structure when the field pushes the charges away from the grafting plane or into a more collapsed structure when the electric field pulls the charges towards the grafting plane. This field-induced transition affects the absorption of Lennard–Jones particles in the brush: in the collapsed state particles only absorb at the brush-solvent interface, while in the stretched state particles mainly absorb into the brush. For the strongest interactions evaluated in this work, we obtained absorption improvements of over 300% between the collapsed and extended state of the coating. This shows great potential for future applications in sensing and separations of small dissolved molecules.

Computational Methods

We performed coarse-grained molecular dynamics simulations on gradient copolymer brushes in an implicit solvent. The simulations were performed in a box with period boundary conditions in the in-plane directions and fixed boundary conditions in the out-of-plane directions. The fixed boundary conditions in the out-of-plane direction are enforced with an harmonic potential with a spring constant of $10^3\ \varepsilon\sigma^{-2}$.

For each brush, the grafting points ($M = 100$) are generated with a desired grafting density of $0.1\ \sigma^{-2}$ using a Poisson disk sampling method;[6] this procedure excludes the influence of a regular lattice on the results. From each grafting point, a chain ($N = 64$) with a gradient in its local charge density is grown so that it is mostly neutral at the grafting interface and mostly charged at its free end. This grafting density and chain length are similar to previous work on polyelectrolyte brushes.[29] Each chain is grown by sequentially appending a bead to the chain; whether the appended bead is charged or neutral is determined based on the ensemble monomer distribution at the relative position along the chain. Here, we use $f(s) = \exp(-(1-s)/0.14)$ where s is the normalized coordinate along the backbone of the polymer; this gives an average charge fraction of $\langle f \rangle = 0.14$.

The particles in the simulation interact via bonded and non-bonded interactions. Bonded interactions are described by a combined finite-extensible non-linear elastic (FENE) and Weeks–Chandler–Anderson (WCA) potential:

$$U_{\mathrm{FENE}}(r) = -0.5KR_0^2 \ln\left(1 - \left(\frac{r}{R_0}\right)^2\right) \tag{2}$$

$$U_{\mathrm{WCA}}(r) = \begin{cases} U_{\mathrm{LJ}}(r) + \varepsilon & \text{for } r \leq 2^{1/6}\,\sigma \\ 0 & \text{for } r > 2^{1/6}\,\sigma \end{cases} \tag{3}$$

$$U_{\mathrm{bond}}(r) = U_{\mathrm{FENE}}(r) + U_{\mathrm{WCA}}(r) \tag{4}$$

where K is $30\ \varepsilon\sigma^{-2}$, R_0 is $1.5\ \sigma$, ε is 1, and σ is 1. This choice of parameters prevents unphysical behavior and bond crossing.[41]

Non-bonded interactions are modeled using a combination of a truncated and shifted 12–6 Lennard–Jones potential for neutral interactions ($U_{\mathrm{LJ,PS}}$) and a Coulomb potential for charged interactions (U_{E}).

$$U_{\mathrm{LJ}}(r) = 4\varepsilon\left(\left(\frac{\sigma}{r}\right)^{12} - \left(\frac{\sigma}{r}\right)^{6}\right) \tag{5}$$

$$U_{\mathrm{LJ,PS}}(r) = \begin{cases} U_{\mathrm{LJ}}(r) - U_{\mathrm{LJ}}(r_c) & \text{for } r \leq r_c \\ 0 & \text{for } r > r_c \end{cases} \tag{6}$$

$$U_{\mathrm{E}}(r) = \frac{Cq_iq_j}{\epsilon r} \tag{7}$$

© 2023 The Authors. ChemPhysChem published by Wiley-VCH GmbH

14397641, 2023, 9, Downloaded from https://chemistry-europe.onlinelibrary.wiley.com/doi/10.1002/cphc.202300003 by University Of Twente Finance Department, Wiley Online Library on [05/12/2023]. See the Terms and Conditions (https://onlinelibrary.wiley.com/terms-and-conditions) on Wiley Online Library for rules of use; OA articles are governed by the applicable Creative Commons License

The cutoff value (r_c) is 2.5 times the σ of a particle for all particles in the simulation. Here, q_i and q_j are the charges on particles i and j, ϵ is the dielectric constant (here $\epsilon = 1$) and C an energy-conversion constant. All long range interactions are calculated using a particle-particle/particle-mesh approach with a relative accuracy of 10^{-4} using an approximation for 2D geometries.[42,43]

The simulation contains five particle types: anchor beads (a, $q = 0$); neutral monomers (m, $q = 0$); charged monomers (c, $q = +1$); counterions (ci, $q = -1$); and target particles (s, $q = 0$). All monomers and the target have the same size ($\sigma = 1.0$); the counterions have a smaller size ($\sigma = 0.5$). The polymer self-interaction ($\varepsilon_{p,p}$) is set to 1.0 to mimic poor solvent conditions. The self-interaction of counterions ($\varepsilon_{ci,ci}$) is set to 0.1 to make charged interaction the dominating interaction of these particles. The self-interaction of the target and the cross-interaction between the target and the polymer are set to the same value ($\varepsilon_{s,p} = \varepsilon_{t,t}$). Multiple sets of simulations are performed where these parameters take the values 0.50, 1.00, 1.25 or 1.50. Cross-interactions between particles that are not explicitly defined are determined based on geometric mixing.

To speed up the equilibration with solvent, we add an excess of target particles to the initial configuration where we add the fewest particles for the weakest target interaction strength and the most for the strongest target interaction strength. This initial configuration is then relaxed using an energy minimization, followed by a run in an NVT ensemble where particle displacements are limited to 0.05 σ with a Langevin thermostat with reduced temperature T^* of 1.0 and a damping factor of 100 dt ($dt = 0.005\ \tau$). The simulation is then run without displacement limitations for 10^5 time steps to further equilibrate the brush. After initial equilibration of the brush, an electric potential is applied normal to the grafting plane so that all charged particles experience a force normal to the grafting plane:

$$F_z = qE_z^* \tag{8}$$

Under these new conditions, the brush is allowed to reorganize for an additional 10^5 time steps.

Next, target is equilibrated with respect to a virtual reservoir with a desired chemical potential ($\mu_s^* = -7$) via a Grand–Canonical–Monte–Carlo (GCMC) approach.[6] The Lennard–Jones vapor is introduced in the simulation box by 10^3 particle insertion/deletion attempts every 10^4 time steps in the MD simulation. Insertion and deletion moves are accepted or rejected based on the Metropolis criterion. Initially, the GCMC exchange is active throughout the full simulation box in order to quickly adjust the number of target particles to near the equilibrium state. This full-box GCMC equilibration is run for 2.0×10^6 time steps. During this full-box GCMC equilibration, particle displacement is limited to 0.05 σ to prevent bond-breaking and lost particles due to insertion of target particles in unfavorable locations. Then, the simulation is continued for 10^6 time steps where the GCMC exchange is limited to the region outside the brush (top 30 σ of the simulation box) during which brush composition stabilizes. Finally, we perform 10^6 time steps to capture the statistics of the system.

We performed various simulations in which we varied the strength of the electric field (E^*) between -15 and $+15$; with an interaction strength of the target ($\varepsilon_{p,t}$ and $\varepsilon_{t,t}$) of 0.50, 1.00, 1.25, or 1.50; and the chemical potential (μ_s^*) of the target of -7. For all simulations a different brush was used to reduce sample bias, but each brush was generated using the same parameters and monomer distribution.

All simulations were performed in LAMMPS.[44,45]

Acknowledgements

This publication is part of Target 5 of the TTW Perspectief research programme ReCoVR: Recovery and Circularity of Valuable Resources which is (partly) financed by the Dutch Research Council (NWO). NWO and SURFsara are acknowledged for HPC resources and support (project ref EINF-2826). The authors acknowledge Leonid Dorogin for carefully reading the manuscript and providing suggestions for improvement.

Conflict of Interest

The authors declare no conflict of interest.

Data Availability Statement

The data that support the findings of this study are available in the online repository 4TU.ResearchData. DOI: 10.4121/21803379.

Keywords: absorption · electric switching · molecular dynamics · polyelectrolyte brush · responsive

[1] C. J. Galvin, M. D. Dimitriou, S. K. Satija, J. Genzer, *J. Am. Chem. Soc.* **2014**, *136*, 12737.
[2] C. J. Galvin, J. Genzer, *Macromolecules* **2016**, *49*, 4316.
[3] L. Sun, B. Akgun, R. Hu, J. F. Browning, D. T. Wu, M. D. Foster, *Langmuir* **2016**, *32*, 5623.
[4] R. A. Gumerov, I. I. Potemkin, *Polym. Sci. Ser. C* **2018**, *60*, 66.
[5] M. Brió Pérez, M. Cirelli, S. de Beer, *ACS Appl. Polym. Mater.* **2020**, *2*, 3039.
[6] G. C. Ritsema van Eck, L. B. Veldscholte, J. H. W. H. Nijkamp, S. de Beer, *Macromolecules* **2020**, *53*, 8428.
[7] L. A. Smook, G. C. Ritsema van Eck, S. de Beer, *Macromolecules* **2020**, *53*, 10898.
[8] M. L. Bruening, D. M. Dotzauer, P. Jain, L. Ouyang, G. L. Baker, *Langmuir* **2008**, *24*, 7663.
[9] L. I. Klushin, A. M. Skvortsov, A. A. Polotsky, S. Qi, F. Schmid, *Phys. Rev. Lett.* **2014**, *113*, 068303.
[10] S. Endo, S. T. J. Droge, K.-U. Goss, *Anal. Chem.* **2011**, *83*, 1394.
[11] E. Aliyev, S. Shishatskiy, C. Abetz, Y. J. Lee, S. Neumann, T. Emmler, V. Filiz, *Adv. Mater. Interfaces* **2020**, *7*, 2000443.
[12] T. M. Birshtein, Y. V. Lyatskaya, *Macromolecules* **1994**, *27*, 1256.
[13] L. A. Smook, G. C. Ritsema van Eck, S. de Beer, *ACS Appl. Polym. Mater.* **2021**, *3*, 2336.
[14] X. Guo, X. Wang, X. Zhou, X. Kong, S. Tao, B. Xing, *Environ. Sci. Technol.* **2012**, *46*, 7252.
[15] L. A. Smook, G. C. Ritsema van Eck, S. de Beer, *J. Chem. Phys.* **2021**, *155*, 054904.
[16] I. Glišić, G. C. Ritsema van Eck, L. A. Smook, S. de Beer, *Soft Matter* **2022**, *18*, 8398.
[17] K. Nagase, J. Kobayashi, A. Kikuchi, Y. Akiyama, H. Kanazawa, T. Okano, *Biomacromolecules* **2008**, *9*, 1340.
[18] K. Nagase, J. Kobayashi, A. Kikuchi, Y. Akiyama, H. Kanazawa, T. Okano, *Biomaterials* **2011**, *32*, 619.
[19] C. Moreno-Castilla, *Carbon* **2004**, *42*, 83.
[20] D. Heine, D. T. Wu, *J. Chem. Phys.* **2001**, *114*, 5313.
[21] D. Meng, Q. Wang, *J. Chem. Phys.* **2011**, *135*, 224904.
[22] Y. Chen, H. Li, Y. Zhu, C. Tong, *J. Phys. Condens. Matter* **2016**, *28*, 125101.
[23] H. Ding, C. Duan, C. Tong, *J. Chem. Phys.* **2017**, *146*, 034901.
[24] H. Ouyang, Z. Xia, J. Zhe, *Nanotechnology* **2009**, *20*, 195703.
[25] Q. Cao, C. Zuo, L. Li, G. Yan, *Biomicrofluidics* **2011**, *5*, 044119.
[26] T. Yamamoto, P. A. Pincus, *EPL* **2011**, *95*, 48003.

© 2023 The Authors. ChemPhysChem published by Wiley-VCH GmbH

14397641, 2023, 9, Downloaded from https://chemistry-europe.onlinelibrary.wiley.com/doi/10.1002/cphc.202300003 by University Of Twente Finance Department, Wiley Online Library on [05/12/2023]. See the Terms and Conditions (https://onlinelibrary.wiley.com/terms-and-conditions) on Wiley Online Library for rules of use; OA articles are governed by the applicable Creative Commons License

[27] Y.-F. Ho, T. N. Shendruk, G. W. Slater, P.-Y. Hsiao, *Langmuir* **2013**, *29*, 2359.
[28] C. Tong, *J. Chem. Phys.* **2015**, *143*, 054903.
[29] H. Merlitz, C. Li, C. Wu, J.-U. Sommer, *Soft Matter* **2015**, *11*, 5688.
[30] T. Pial, M. Prajapati, B. Chava, H. Sachar, S. Das, *Macromolecules* **2022**, *55*, 2413.
[31] T. Hüffer, T. Hofmann, *Environ. Pollut.* **2016**, *214*, 194.
[32] M. M. Alam, K. S. Jack, D. J. Hill, A. K. Whittaker, H. Peng, *Eur. Polym. J.* **2019**, *116*, 394.
[33] T. Gleede, J. C. Markwart, N. Huber, E. Rieger, F. R. Wurm, *Macromolecules* **2019**, *52*, 9703.
[34] Z. Wang, T. Liu, Y. Zhao, J. Lee, Q. Wei, J. Yan, S. Li, M. Olszewski, R. Yin, Y. Zhai, M. R. Bockstaller, K. Matyjaszewski, *Macromolecules* **2019**, *52*, 9466.
[35] J. Zhang, B. Farias-Mancilla, M. Destarac, U. S. Schubert, D. J. Keddie, C. Guerrero-Sanchez, S. Harrisson, *Macromol. Rapid Commun.* **2018**, *39*, 1800357.
[36] E. M. Stuve, *Chem. Phys. Lett.* **2012**, *519–520*, 1.
[37] S. V. Venev, I. I. Potemkin, *Soft Matter* **2014**, *10*, 6442.
[38] V. S. Kravchenko, I. I. Potemkin, *J. Phys. Chem. B* **2016**, *120*, 12211.
[39] J.-M. Y. Carrillo, A. V. Dobrynin, *Langmuir* **2009**, *25*, 13158.
[40] G.-L. He, H. Merlitz, J.-U. Sommer, *J. Chem. Phys.* **2014**, *140*, 104911.
[41] K. Kremer, G. S. Grest, *J. Chem. Phys.* **1990**, *92*, 5057.
[42] I.-C. Yeh, M. L. Berkowitz, *J. Chem. Phys.* **1999**, *111*, 3155.
[43] V. Ballenegger, A. Arnold, J. J. Cerdà, *J. Chem. Phys.* **2009**, *131*, 094107.
[44] S. Plimpton, *J. Comput. Phys.* **1995**, *117*, 1.
[45] A. P. Thompson, H. M. Aktulga, R. Berger, D. S. Bolintineanu, W. M. Brown, P. S. Crozier, P. J. in 't Veld, A. Kohlmeyer, S. G. Moore, T. D. Nguyen, R. Shan, M. J. Stevens, J. Tranchida, C. Trott, S. J. Plimpton, *Comput. Phys. Commun.* **2022**, *271*, 108171.

Manuscript received: January 2, 2023
Revised manuscript received: January 27, 2023
Version of record online: February 22, 2023

© 2023 The Authors. ChemPhysChem published by Wiley-VCH GmbH

14397641, 2023, 9, Downloaded from https://chemistry-europe.onlinelibrary.wiley.com/doi/10.1002/cphc.202300003 by University Of Twente Finance Department, Wiley Online Library on [05/12/2023]. See the Terms and Conditions (https://onlinelibrary.wiley.com/terms-and-conditions) on Wiley Online Library for rules of use; OA articles are governed by the applicable Creative Commons License